Journal of Physics: Conference Series

PAPER • **OPEN ACCESS**

40 year anniversary of the RADAN systems – compact pulsed power sources for various investigations

To cite this article: V G Shpak *et al* 2021 *J. Phys.: Conf. Ser.* **2064** 012002

View the article online for updates and enhancements.

This content was downloaded from IP address 45.82.99.47 on 26/11/2021 at 03:05

40 year anniversary of the RADAN systems – compact pulsed power sources for various investigations

V G Shpak[1], S A Shunailov and M I Yalandin

Institute of Electrophysics, UB, RAS, 620016, Yekaterinburg, Russia

[1] Corresponding author's e-mail: radan@iep.uran.ru

Abstract. This article includes a brief overview of the compact RADAN-series subgigawatt pulsed voltage sources and describes their capabilities in various electrophysical researches. We present the results obtained in the experiments at nano- and subnanosecond time scales on the formation of the voltage pulses with a special shape, electron beams emission in air gaps and by the cold cathodes in vacuum, as well as generation of electromagnetic radiation. Particular attention is paid to the promising application of the RADAN systems.

1. Introduction

The creation background of the high-voltage RADAN generators is associated with the discovery of explosive electron emission (EEE) in the 1970s [1] and the development of a new element base: sealed-off pulsed X-ray tubes [2] and high-voltage high-pressure gas dischargers [3] specifically for compact nanosecond X-ray devices [4]. The use of these devices for flaw detection (defectoscopy) required reducing the dimensions of high-voltage blocks, their tightness and eliminating the dependence of their characteristics on the surrounding metal, in particular small cross-section pipes, which represented a closed loop for a coreless high-voltage pulse transformer.

We did not consider Marx generators as an alternative to transformer devices due to the large number of spark switches and low-inductive capacitors in serial stages. The most adequate scheme was presented with an energy storage device in the form of a high - voltage coaxial capacitor, a pulse forming line (PFL) (figure 1a), combined with a Tesla transformer having open magnetic core [5]. With a sufficient length, the outer and inner parts of the magnetic core provide a high connection between the transformer windings mounted in the oil-filled PFL gap. The parts of such core assembled from insulated steel plates simultaneously serve as conductors of the coaxial line, but the azimuthal current is excluded, thus, the short circuit is eliminated. This made it possible to place the high-voltage storage device in a closed sealed metal case. So, the level of electromagnetic interference was significantly reduced, and with the gas spark gap quickly switching on (*S* in figure 1a) the voltage pulse, formed into a matched load, had a quasi-rectangular shape (figure 1b). These properties turned out to be fundamentally important not only for X-ray sources, but also for the creation of scientific equipment, where nanosecond high-voltage pulses with a flat top and electron beams with a predominance of particles with a certain energy were required.

2. Basing pulsed power units

There are many features that distinct high voltage blocks of the most compact encapsulated RADAN sources (*1-4* in figure 1d) from their larger prototypes and SINUS-series devices [6] that also use a

Content from this work may be used under the terms of the Creative Commons Attribution 3.0 licence. Any further distribution of this work must maintain attribution to the author(s) and the title of the work, journal citation and DOI.
Published under licence by IOP Publishing Ltd

Tesla transformer (TT, figure 1c) as a PFL charger. First of all, desirable light weight dictates rejection of the pressure equalizing in the PFL isolating oil with the gas pressure (tens of atmospheres) in the spark discharger. This does not represent problem when a standard sealed-of high-voltage discharger *S* is used. The second measure is placement of TT primary circuit, i.e., capacitor C_1 and spark discharger S_1 (type P-28, self-breakdown at 2.5 kV) inside the same encapsulated cylindrical case. Also, to charge C_1, a remote, long-cable connecting voltage converter (*5*) is used. There are two options of this converter: AC-DC (220 V mains – 3 kV DC output) or DC-DC (12 V car battery - 3 kV DC output).

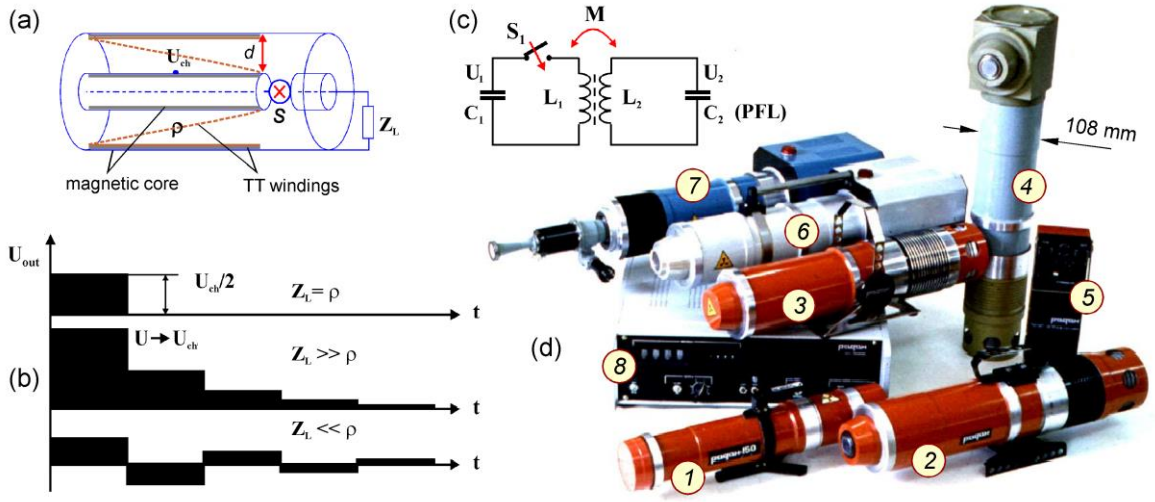

Figure 1. The first generation of the RADAN-series apparatus. (a) Design of the PFL with a built-in components of the TT. (b) Discharge regimes of the PFL. (c) Simplified circuit of the TT. (d) Compact RADAN-type devices used in various scientific and practical applications since 1981 by now: *1-3* – X-ray apparatus operating at 10 pps; *4* and *6* – sources of electron beam (2 ns; ≈ 200 keV; ≈ 1 kA/cm^2) extracting into the air for radiation-effect tests; *5* and *8* – charging devices; *7* – Compact burst-operating 70-GHz backward-wave oscillator (BWO): 1.5 ns; ≈ 10 MW; 10 pps.

A rather high voltage of C_1 (with combined paper-film dielectric) charging is a measure aiming to reduce the PFL charging time to ≈ 1 μs which is a strict requirement to prevent a surface flashover of ceramic insulators used in the standard high-pressure gas dischargers *S*, serial types P-43 (150 kV) (*1*) and P-49 (240 kV) (other devices in figure 1d). Even higher C_1 charging of up to 5 kV (charging supply *8*) is used in the apparatus *6* and *7*, which can operate in synchronizing mode by triggering the primary switches S_1, namely three-electrode controlled discharger P2-65 (*7*) providing a microsecond spread, and a hydrogen thyratron TGI-1-100/8 possessing a ≈ 1 ns switching accuracy. For the last case, output pulse of the device *6* has a time jitter of tens of nanosecond which is determined by uncontrolled high-voltage discharger P-49.

Depending on the output load, 2-3-ns-long pulses produced by the devices shown in figure 1d had a voltage amplitude in the range of 150 – 250 kV. Alongside X-ray sealed-off vacuum tubes IMA2-150D, IMA5-320D (devices *1-3*), a vacuum diode with beryllium-foil (150 μm) window (*4* and *6*) were widely used in a variety of experiments on plasma-chemistry, radio-biology, radiation physics, etc., wherever short powerful electron beams extracting into air were necessary to produce non-thermal, high-power effects onto irradiated objects.

To expand the applications of compact high-voltage generators in laboratory practice, multi-functional devices were developed in the 1990s. This is the basic RADAN-303 source (hereafter driver) [7] in the form of an integrated unit (figure 2a), including a resonant charging device for the capacitor C_1 in the first TT circuit, a thyristor switch S_1 with a start system and, in fact, a high-

voltage capacitive storage device in the form of a pulsed double forming line (PDFL) shown in figure 2b. A design feature of the PDFL is a slightly different length of the internal and external coaxial lines. The calculation shows [8] (figure 2c) that when such a PDFL is discharged, the output pulse has an irregular shape.

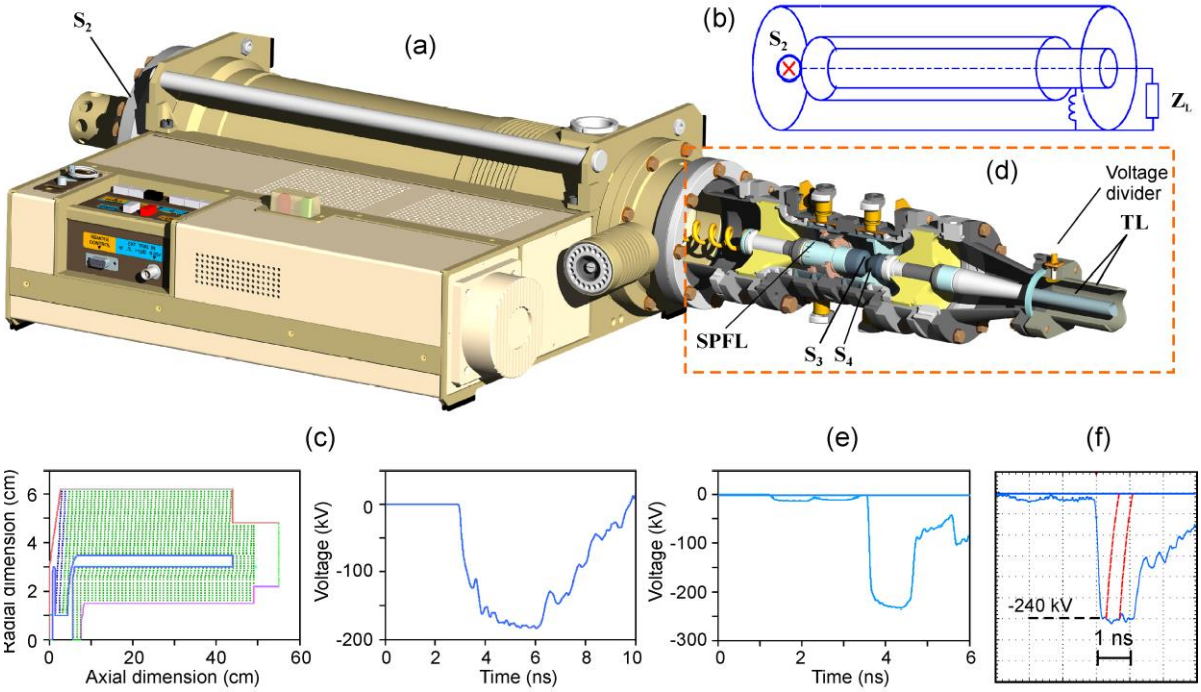

Figure 2. (a) RADAN-303 pulsed source based on the PDFL scheme (b). Geometry of the PDFL pulser and numerical simulation of an output ≈ 4-ns pulse formation (c). (d) Inductive-capacitive converter with an output gas discharger and modeling of its operation for the further pulse compression (e). (f) Experimental waveform of compressed pulses at 45-Ohm output TL.

The noted disadvantage is eliminated by using an inductive-capacitive converter (figure 2d) [9], that has the same output impedance (45 Ohm) as the PDFL driver (2x22.5 Ohm), but, at the same time, increases the amplitude of the output pulse, equalizes the voltage pulse top and shortens its duration – depending on the electrical length of the additional short pulse forming line (SPFL). Figure 2e shows the calculation of pulse compression (figure 2c) and the experimental waveform (figure 2f) of the output pulse obtained after the operation of the high-pressure gas switch S_3 (N_2; H_2, pressure of up to 100 atm). Thus, voltage pulses with a front of hundreds of picoseconds and an amplitude of (200-300) kV are obtained at the SPFL output when the PDFL charging up to 150-220 kV. If a cutting spark gap S_4 [10] is installed in the converter unit, the output pulse duration (FWHM) can be shortened to ≈ 300 ps without reducing the amplitude, as conventionally shown by the dotted lines in figure 2f. Due to the presence of a pass-through interelectrode capacitance of the spark gap S_3, the output voltage pulse with a short front is always preceded by a nanosecond pre-pulse, which is a derivative of the driver pulse front until the moment of S_3 breakdown. Note that the spark gaps of the S_3 and S_4 switches can be precisely changed with the help of eccentric gears without depressurization. This allows one to quickly adjust the parameters of the output pulses in the experiments.

Instead of or in addition to the gas-discharge pulse converter, a solid-state one can be used, representing a coaxial transmission line with ferrite filling in the insulation gap (figure 3a), which is magnetized by an axial field H_z from an external dc solenoid [11]. Such a gyromagnetic non-linear transmission line (NLTL) provides in the passive mode ($H_z = 0$) a sharpening of the driver pulse

front (*1* in figure 3b), and with magnetization ($H_z \neq 0$) and a sufficient length of NLTL, the excitation of high-frequency modulation of the voltage envelope (*2* in figure 3b). This modulation leads to a further shortening of the voltage front, and in case of limiting the duration of the incident pulse, to the formation of a dedicated subnanosecond peak of increased amplitude (figure 3c). It is important to note that by varying the current in the solenoid winding, it is possible to precisely shift the pulse front: typically 1 ps / 10 mA.

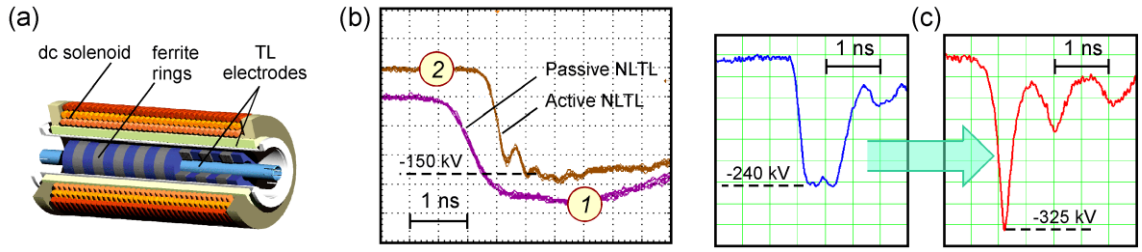

Figure 3. (a) Schematic of the NLTL. (b) Sharpening of the pulse leading edge by switching-on magnetization of the ferrite insertion. (c) NLTL as the second-stage compressor of the pulse produced by the gas-discharge converter shown in figure 2d.

The capabilities of the driver described above and experimental installations based on it are significantly expanded due to the specifics of the PDFL S_2 high-voltage switch. Since the output pulses of negative polarity are mainly required, the intermediate PDFL electrode is charged to a positive potential. It is important that the S_2 switch is located between the intermediate and external (grounded) electrode of the PDFL. This allows to use a simple mechanical adjustment of the spark gap under the pressure, thereby changing the self-breakdown voltage. In addition, a short negative trigger pulse can be easily supplied through the grounded cathode electrode (figure 4a). The idea of obtaining a precision control was the subnanosecond accuracy of S_2 switching, if you create conditions for a leading breakdown (*1* in figure 4b) during a short triggering pulse (figure 4c). The accuracy of the starting pulse coming (this is usually tens of nanoseconds) against the background of an 8-microsecond PDFL charge time ensures the amplitude stability of the driver pulse. If the starting pulse is split into several channels, then the nanosecond output pulses of independent drivers (figure 2c), as well as shorter pulses (figure 2f) can be synchronized with subnanosecond accuracy (figure 4c).

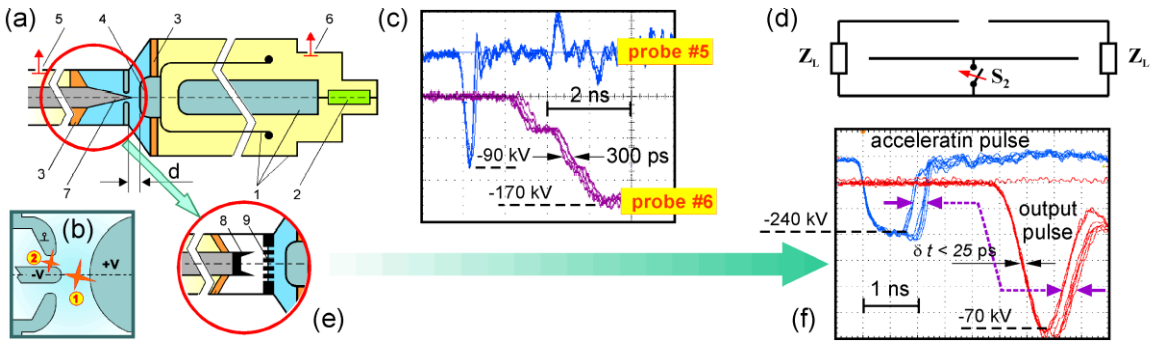

Figure 4. (a) Schematic of PDFL with a three-electrode triggering gas discharger. *1* – DPFL electrodes; *2* –load; *3* – insulators; *4* – anode of the spark gap; *5*, *6* – voltage probes; *7* – triggering electrode; *8* – graphite cathode; *9* – foil window. (b) Sequence of breakdowns providing precision triggering. (c) – Triggering short pulse and PDFL switching response. (d) Schematic for two PDFLs switching by a common discharger S_2. (e) Triggering of S_2 by injected electron beam. (f) Accelerating pulse supplying the EEE cathode in option (e) and output (response) pulse of PDFL.

A special experiment [12] on switching a spark gap with a high-current electron beam with a subnanosecond front (figure 4e) showed the possibility of even more accurate activation of the RADAN PDFL driver (figure 4f). The total switching time spread of ≈ 25 ps, according to the "three sigma" rule, corresponds to a standard deviation of < 5 ps. It turned out, however, that the high-voltage source of the electron beam should be comparable in power to the driver being started. That is, to create multi-channel systems with precision synchronization, splitting the signal of one powerful driver is energetically more effective.

3. Diagnostics

To determine the characteristics of the pulses at the output of the driver and converters, the probes that provide a resolution adequate to subnanosecond band are needed. The same applies to measurements of electron beam currents, registration of microwave pulse envelopes, and high-frequency filling of radio pulses. Note the specifics of transmission ducts and loads operating in the duration range of units of nanoseconds (FWHM) and much less. Firstly, these are small transverse dimensions, which are required to transmit even shorter pulse edges. Secondly, some types of probes turn out to be inapplicable, for example, Rogowski coils, resistive current shunts and voltage dividers, where the components used can no longer be considered lumped and they generate reflections. Thirdly, the probes cannot be placed near miniature high-potential vacuum load elements, such as a cathode. Finally, in complex measurements of the supply pulse and the current of electron beam or the current in the discharge gap, it is rather difficult to synchronize the data obtained by spaced (remote) sensors. The delay between signals, as a rule, includes the process under investigation.

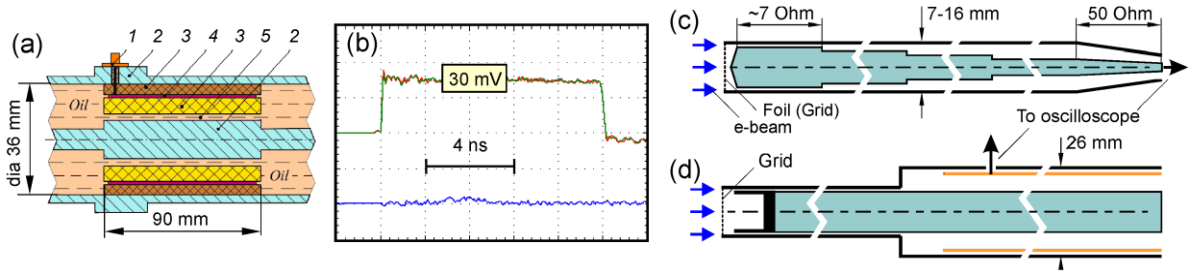

Figure 5. (a) Sketch drawing of the capacitive voltage divider on coupled coaxial lines: *1* – SMA stub connector; *2* – electrodes of TL; *3* – Teflon tubular insulators; *4* – thin cylindrical electrode (sensor); *5* – oil gap. (b) Low-decay response of the divider (a) onto calibration pulse (rise time 80 ps). (c) A picosecond-response collector probe of e-beam current. (d) Probe of high-current, nanosecond e-beam currents equipped with a Faraday-cup collector.

Taking into account the noted specifics, to register short voltage pulses in transmission lines (TL), we have specially developed capacitive dividers with an “umbrella” sensor of a small area (“Voltage divider” in figure 2d) or an even smaller end-face version. In some cases, dividers on coupled coaxial lines turned out to be convenient (figure 5a), where an increased capacitance of the sensor to the grounded electrode of TL determines a large differentiation constant (figure 5b) and does not give the effect of shelf modulation and front extension due to delay of the reflections. A separate goal is the creation of sensors with a high division factor and their adjustment.

Collector probes are used to measure the current of electron beams behind the anode of vacuum and gas diodes. Depending on the current pulse duration, the collector is a profiled end face of a low-resistance (6-7 Ohm) coaxial line (for the pulses < 100 ps) or a Faraday cup mounted at this end face (for nanosecond pulses). In the first case (figure 5c), a stepped transition to a 50-ohmic cable is used for registration. In the second variant (figure 5d), the line impedance increases abruptly to tens of Ohm, and in this section a capacitive divider on coupled lines is installed. In the probe of picosecond

current pulses, collector is always shielded by a fine mesh or foil that is transparent for the electrons of the analyzed energies. In the nanosecond version, a grid and/or radially slotted collimators are used, which reduce recorded current to an acceptable level. Note that the developed probes allow recording the kiloampere currents of nano- and subnanosecond explosive emission beams, as well as ampere fluxes of runaway electrons in a gas diode with duration of up to 10 ps.

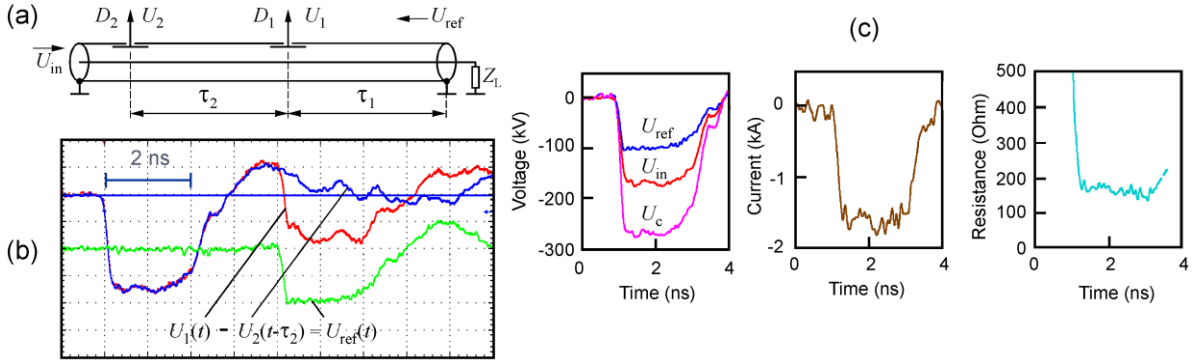

Figure 6. (a) Scheme of the dynamic time-domain reflectometry and typical set of waveforms (b) providing a complete information for evaluations of the cathode (load) voltage (U_c), emissive current and the load resistance (c).

The papers [13, 14] describe a diagnostic method (dynamic time-domain reflectometry, DTDR), specifically developed for the analysis of fast processes in gas-discharge and injection loads of high-voltage RADAN series generators with additional pulse compression devices. For the pulse duration $\tau_p \approx 2$ ns or shorter, it is convenient to use the measurement scheme shown in figure 6a, where the signal delay between two identical voltage probes D_1 and D_2 is not so significant ($\tau_2 \approx \tau_p$) that due to losses in the TL their signals U_1 and U_2 were different. If these signals are subtracted considering the time shift (figure 6b), then the reflected signal U_{ref} is determined without noise overlap (tail of the incident pulse U_{in}). When TL is uniform from the probes to the load (without parasitic reflections), then U_{ref} makes a correct information about dynamics of processes in the load. If you measure the delay τ_1 in the no-load mode or short circuit at the TL end, then a comparison of U_{in} and U_{ref} accounting the characteristic impedance of TL, gives the voltage across the load U_c, the current in it I_d and the dynamic impedance Z_L (figure 6c). In the case of electron injectors, the voltage and current of the cathode emission are determined in this way. The listed parameters are measured in just one pulse and have absolute synchronization, which is of fundamental importance in studies of emission and discharge processes.

4. Advanced experiments

4.1. Desktop repetitive sources of power electron beams for lab investigations

During the first two decades of operation of the RADANs (see, e.g., [15-17] and citation therein), researches on the formation of nanosecond explosive-emission electron beams for radiation-technological applications was developed [18]. The practice of using high-voltage pulse sources has shown that with a decrease in the pulse duration shorter than 5-7 ns, a rather noticeable increase in the electric strength of almost all types of insulation takes place. This allows decreasing the size of the created devices, to reduce the requirements for the working vacuum. On the basis of RADAN sources, a number of small-sized accelerators were developed (table 1) with the extraction of an electron beam into the atmosphere through a foil window (figure 7). In ribbon diodes, an explosive-emission electron beam appears behind the foil with a small delay with respect to the leading edge of the voltage wave traveling along the diode as along a line. To operate these diodes, a pressure of 10^{-1} Tor provided by a rotary pump is sufficient. With a subnanosecond traveling voltage pulse duration,

the ribbon diode can operate at atmospheric pressure - with a thin foil or mesh window. In this case, the beam will represent a short (< 50 ps) burst of runaway electrons traveling along the diode window at the speed of light.

Table 1. Specification of RADAN accelerators equipped with various e-beam diodes.

Parameter	IMA3-150E ((sealed-off)	Ribbon diodes (pumped)		
Cross section of e-beam near the foil window (mm)	15 (dia)	5 x 60	5 x 110	5 x 480
Peak current, in air (kA)	1	1.2	1.8	1
Foil material, thickness (μm)	Be, 200	Al-Be, 40	Al-Be, 40	Al-Be, 60
Peak accelerating voltage (kV)	250	180	200	200
Maximal reprate (p.p.s.)	25	25	100	100
Pulse width (ns)	4	4	4	3

(a) (b) (c)

Figure 7. Compact accelerators based on the sealed-off (a), pumped ribbon (b) vacuum diodes and air-filled diode with travelling runaway electron bunch (c).

4.2. Runaway electrons in gas gaps and associated breakdown effects

Researches with the use of RADAN compact high-voltage technique and diagnostic devices can be divided into two stages, the conditional boundary between which in the early 2000s is associated with the advent of real-time digital oscilloscopes with a registration bandwidth of up to 10 GHz and higher. This has opened up new opportunities in the fast processes researches as well as for the generation of high-power microwaves (HPM). An example of the effective use of RADAN sources in the experiments with picosecond resolution is the study of the effects of continuous electron acceleration (runaway) in dense gases. In these studies, a fundamental role was played by the technical possibilities of tuning the parameters of a high-voltage pulse (figure 2f) applied to the discharge gap with a sharply inhomogeneous distribution of the electric field between the cathode and anode: amplitude, duration (FWHM), and front steepness.

A review article [19] provides data on the possibilities of controlling the voltage and the moment of runaway electrons (RAE) emission at the leading edge of high-voltage pulse, depending on the change in electric field amplification at the cathode, where it must exceed the critical value (E_c) for the runaway of thermal electrons at the boundary of near-cathode plasma. Later, a runaway criterion was obtained [20], which is valid not only in the region of the field amplification, but also in the rest of the air gap, where $E < E_c$. The data on the runaway conditions made it possible to create a RAEs source with two-gap electrode system, where emission moment is stabilized up to a few picoseconds at the initial section of the voltage leading edge, and the particle energy at the anode is set by the high-voltage pulse amplitude (figure 8a). For this, a pulse was applied to the near-cathode gap with a delay on the order of the voltage rise time [21]. Later, using a megavolt driver with solid-state

switches, the developed approach to controlling the RAEs emission moment made it possible to obtain a particle flux with the energy at the anode of > 1.4 MeV [22].

The experiment [23] on determining the duration of the "elementary" RAE flow from the tip of a conical cathode was of fundamental importance. Here, direct measurements have shown (figure 8b) that the observed current duration ≈ 10 ps (FWHM) represents an upper evaluation, which is determined by the characteristics of the current probe and transient response of the oscilloscope. This meant that RAEs flow in the electrode gap can be described as a thin diverging layer, but not as a beam. It has also been suggested that there are asynchronous emission of multiple RAEs flows from different regions of the cathode with an elongated edge, as a result of which the integral current at the anode lasts longer. This was confirmed by continuing the experiment [24] with a magnetized RAEs flux, which is discussed in a separate paper [25].

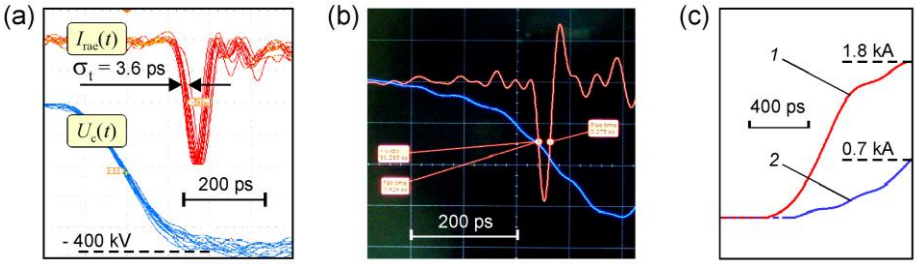

Figure 8. (a) Stabilization of the RAEs emission instant at the fast section of the voltage pulse leading edge. (b) Current pulse of the RAEs (≈ 10 ps FWHM) emitting in the vicinity of a sharp-edge conical cathode. (c) Difference in the air gap breakdown currents rise rate and amplitudes for the case of advanced RAEs emission (*1*) and their absence (*2*).

Considerable attention was paid to the experiments on initiation breakdowns in an air gap by a flow of runaway electrons. Here we used the capabilities of the reflectometric method (see Section 3), which turned out to be the most effective in studying the radial breakdowns of the gap of coaxial TL in the field of traveling voltage pulse. In [26], the increase in the breakdown current rise rate in the discharge gap during RAEs emission was analyzed in detail (figure 8c), and in the experiments [27], a regime was demonstrated when, even with the RAEs emission, no distortions of the traveling voltage pulse occurs due to the limited amplitude and duration of the voltage.

4.3. RADAN devices in the HPM applications

A widespread version of high-current electron injectors are sources of tubular beams formed in vacuum magnetically insulated coaxial diodes (MICDs) [28]. Such beams were used to generate microwave pulses in the Ka-band, including the generation in the superradiance (SR) mode. The results in this field [29-32] stimulated similar studies in the X-band and further improvement of the sources of subnanosecond Ka-band SR pulses of gigawatt power level [33, 34].

Research on the HPM generation took full capabilities of the pulse compression device described in Section 2. In particular, sharpening switch S_3 of the converter shown in figure 2d, when filled with hydrogen at a pressure of 100 atm, showed high switching stability without gas circulation up to repetition rates of 1-3.5 kHz. As a result, after the test of the RADAN-based SR BWO [35], the SR pulse stability attained in the experiment [36] was sufficient for stroboscopic registration (figure 9a). That is, a stable switching of the spark gap determines stability of the cathode emission [37], beam current, and radiation of HPM source. Studies of this relationship [38, 39] remain relevant [40], and have led to date to the demonstration of the HPM generation mode [41-46], where the radiation phase is fixed, since it is given by a seed signal from a stable leading edge of the beam current [47] or external radio pulse.

In the previous context, the experiment with two RADAN-type PDFL drivers (figure 9b), where spark gaps S_2 are combined (see layout in figure 4d), is interesting. Here, two identical voltage pulses (figure 9c) are applied to the cathodes synchronously and a coherent summation of nanosecond Ka-band microwave pulses (*ibid*) is achieved [48]. Since the power density at the interference maximum of radiation pattern (figure 9d) increases quadratically to the number of sources, the electric field in the wave beam can be many times higher than the static breakdown field for the gas. Nevertheless, experiment [42] showed that in the fields of SR pulse with a duration of ≈ 200 ps (FWHM) and a power of ≈ 600 MW, breakdown of air near vacuum window of the microwave generator turns out to be incomplete (delayed). Therefore, the microwave pulse outputs into ambient air with low distortion. If the field strength is increased by decreasing diameter of the waveguide channeling the HPM pulse, a consistent drop in power and shortening of transmitted microwave pulse are observed. These data (figure 9e) obtained for the Ka-band SR pulse [49], allowed an alternative assessment of the registered power for the SR-source of the frequency range ≈ 90 GHz [50] by the threshold of air breakdown in the microwave field (figure 9f).

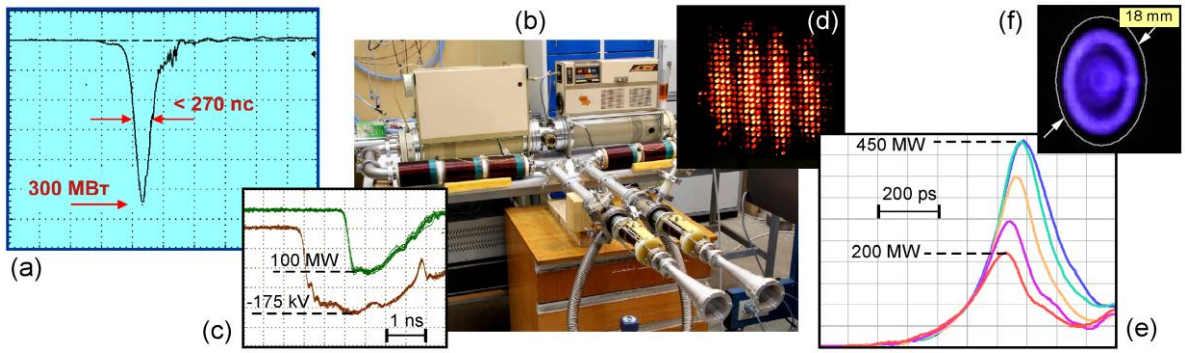

Figure 9. (a) Stroboscopic record of Ka-band SR pulse. (b) RADAN drivers with a common gas discharger feeding two Ka-band BWOs. (c) Waveforms of accelerating voltage pulses and ten stored summarized microwave pulses (100 MW each). (d) Radiation pattern of summarized microwave beams. (e) Shortening in the duration and power decay of SR pulse with a decrease in the diameter of transmitting waveguide. (f) Microwave air breakdown in the field of a 90-GHz wave TM_{01}.

4.4. Prospective experiment

An increase in the breakdown strength with a shortening of the exposure of a strong microwave field is known for both gaseous and vacuum media. For instance, at field strength of 2 MV/cm, a 2-GW pulse of the Ka-band SR BWO [51] was extracted from slow-wave structure (SWS) without distortions due to delay of the EEE-plasma development and expansion. This effect can be used for the pumping of a half-wavelength, low-Q microwave cavity, type “pill-box”, for high-gradient acceleration (HGA) of electrons by the Ka-band SR pulse [34]. In this experiment, the RADAN drivers need to be synchronized (figure 4c) to implement two-channel scheme shown in figure 10a. Its peculiarity is that it is difficult to place the components for time-domain diagnostics of accelerated electron bunches in the accelerating channel. Therefore, their energy can be estimated from the bremsstrahlung of the beam from the collector.

An alternative is a scheme with one high voltage driver (figure 10b), where feeding pulse (as in figure 6b) is applied to two coaxial graphite cathodes. The outer cathode emits a tubular beam that generates SR pulse counterpropagating to electrons (BWO-type interaction). "Used" electrons go to the collector along the lines of force of the solenoid magnetic field. An internal paraxial beam with initial energy of 300 keV passes into the hole in the half-wavelength cavity and is accelerated. Calculation [8] shows (figure 10c) that at a peak SR power of about ≈ 0.8 GW, the longitudinal field of the TM_{01} wave at the cavity pump peak can modulate paraxial beam with a current of 100-200 A

up to the energy of 2 MeV. That is, the increase in kinetic energy achieves ≈ 1.7 MeV, and for acceleration region length of ≈ 0.4 cm, acceleration gradient exceeds 400 MV/m.

The train of paraxial accelerated bunches is forwarded out of SWS into the zone of registration by a collector probe equipped with a high-energy pass filter. It is assumed that the probe similar to that shown in figure 5c will provide a time-resolved registration of the bunches following with the interval approximately equal to the period of SR pulse oscillations (≈ 25 ps). Time response of the probe can be calibrated with a 10-ps flow of magnetized runaway electrons by analogy with the experiment [23] mentioned in Section 4.1.

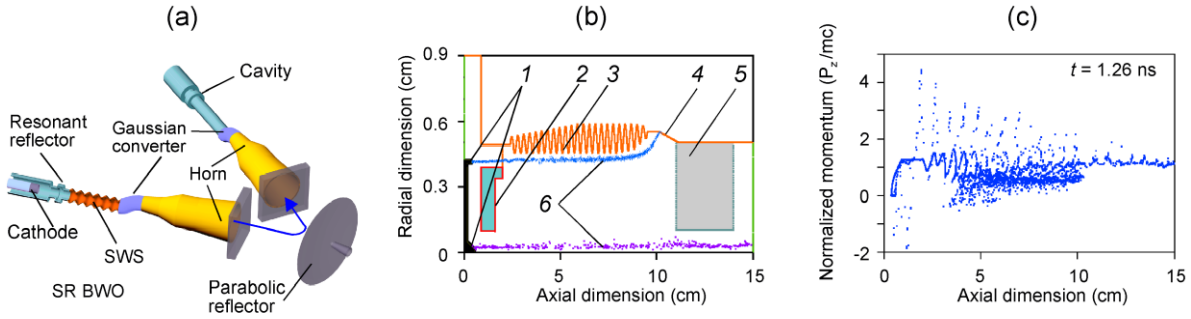

Figure 10. (a) Two-channel scheme for HGA using precisely synchronized RADAN-type drivers. (b) Geometry of the particle-in-cell simulation [8] for a single-channel option of HGA experiment. (c) Phase portrait (dependence of a normalized longitudinal momentum on the axial coordinate) for coaxial beams. *1*- cathodes; *2*- cavity; *3*- SWS; *4*- collector; *5*- microwaves absorber; *6*- e-beams.

5. Conclusion

Summarizing, the pulsed power sources of RADAN series have been successfully used for many years to study fast-flowing electrophysical processes in gases and vacuum. Simple and reliable in operation, they have become also an effective tool in various related fields of scientific researches and have a chance to provide the further breakthrough scientific results. RADAN-series pulsers produce low interferences, do not require highly qualified personnel, specially equipped rooms and are safe in operation. These features are highly promising also for interdisciplinary applications.

Acknowledgments

The equipment of the Collective Use Center at the Institute of Electrophysics, UD, RAS has been used in the experiments. This work in part of the RADAN-based systems prospective application for high-gradient electron acceleration is supported by the Russian Science Foundation, Grant No 21-19-00260.

References

[1] Mesyats G A and Proskurovsky D I. 1971 *JETP Lett.* **13** 7
[2] Belkin N V and Aleksandrovich E G 1972 *Prib. Tekh. Eksp*. **2** 196
[3] Kiselyov Y V and Cherepanov V P 1976 *Spark dischargers* (Moscow: Sov. Radio) p 72
[4] Mesyats G A, Ivanov S A, Komyak N I and Peliks E A 1983 *High-Power Nanosecond X-ray Pulses* (Moscow: Energoatomizdat) p 168
[5] El'chaninov A S, Zagulov F Ya, Korovin S D, Landl' V F, Lopatin V V and Mesyats G A 1983 *High-Pulse-Repetition-Rate, High-Current Electron Beam Accelerators High-Current Pulsed Electron Beams in Technology* (Novosibirsk: Nauka) p 5
[6] Korovin S D, Rostov V V, Polevin S D, Pegel I V, Schamiloglu E, Fuks M I, Barker R J 2004 *IEEE Rad. Conf.* **92** 1082
[7] Shpak V G, Shunailov S A, Yalandin M I and Dyad'kov A N 1993 *Instrum. Exp. Tech*. **36** 106
[8] Tarakanov V P 1992 *User's Manual for Code KARAT* (Springfield: Berkeley Research.

Associates, Inc.)
[9] Yalandin M I, Lyubutin S K, Oulmascoulov M R, Rukin S N, Shpak V G, Shunailov S A and Slovikovsky B G 2002 *IEEE T. Plasma Sci*. **30** 1700
[10] Mesyats G A, Shpak V G, Shunailov S A and YalandinMI 1994 *Proc. SPIE* **2154** 262
[11] Romanchenko I V, Rostov V V, Gubanov V P, Stepchenko A S, Gunin A V and Kurkan I K 2012 *Rev. Sci. Instrum*. **83** 074705
[12] Yalandin M I, Sharypov K A, Shpak V G, Shunailov S A and Mesyats G A 2010 *IEEE T. Dielect. El. In.* **17** 34
[13] Sharypov K A, Shpak V G, Shunailov S A, Ul'masculov M R and Yalandin M I 2013 *Rev. Sci. Instrum*. **84** 055110
[14] Sharypov K A, Ul'masculov M R, Shpak V G, Shunailov S A, Yalandin M I, Mesyats G A, Rostov V V and Kolomiets M D 2014 *Rev. Sci. Instrum*. **85** 125104
[15] Yalandin M I and Shpak V G 2001 *Instrum. Exp. Tech*. **44** 285
[16] Mesyats G A, Korovin S D, Rostov V V, Shpak V G and Yalandin M I 2004 *IEEE Rad. Conf.* **92** 1166
[17] Mesyats G A and Yalandin M I 2005 *Phys. Usp*. **48** 211
[18] Mesyats G A, Shpak V G, Yalandin M I and Shunailov S A 1995 *Radiat. Phys. Chem*. **46** 489
[19] Mesyats G A, Yalandin M I, Reutova A G, Sharypov K A, Shpak V G and Shunailov S A 2012 *Plasma Phys. Rep*. **38** 29
[20] Zubarev N M, Yalandin M I, Mesyats G A, Barengolts S A, Sadykova A G, Sharypov K A, Shpak V G, Shunailov S A and Zubareva O V 2018 *J. Phys.* D *Appl. Phys*. **51** 284003
[21] Mesyats G A, Sadykova A G, Shunailov S A, Shpak V G and Yalandin M I 2013 *IEEE T. Plasma Sci.* **41** 2863
[22] Mesyats G A *et al* 2018 *Appl. Phys. Lett*. **112** 163501
[23] Mesyats G A *et al* 2020 *Appl. Phys. Lett*. **116** 063501
[24] Gashkov M A, Zubarev N M, Zubareva O V, Mesyats G A, Sharypov K A, Shpak V G, Shunailov S. A and Yalandin M I 2021 *J. Exp. Theor. Phys. Lett*. **113** 370
[25] Mesyats G A, Sharypov K A, Shpak V G, Shunailov S A, Yalandin M I and Zubarev N M 2021 *J. Phys. Conf. Ser*. Presented issue.
[26] Sadykova A G. Zubarev N M, Mesyats G A, Osipenko E A, Sharypov K A, Shpak V G, Shunailov S A and Yalandin M I 2020 *Russ. Phys. J*. **62** 2005
[27] Zubarev N M, Kozhevnikov V Yu, Kozyrev A V, Mesyats G A, Semeniuk N S, Sharypov K A, Shunailov S A and Yalandin M I 2020 *Plasma Sources Sci. T.* **29** 125008
[28] Belomyttsev S Ya, Rostov V V, Romanchenko I V, Shunailov S A, Kolomiets M D, Mesyats G A, Sharypov K A, Shpak V G, Ulmaskulov M R and Yalandin M I 2016 *J. Appl. Phys*. **119** 023304
[29] Ginzburg N S *et al* 1997 *Phys. Rev. Lett*. **78** 2365
[30] Ginzburg N S *et al* 1999 *Phys. Rev.* E **60** 3297
[31] Wiggins S M *et al* 2000 *Phys. Rev. Lett*. **84** 2393
[32] Ginzburg N S *et al* 1997 *Nucl. Instrum. Meth.* A **393** 352
[33] Eltchaninov A A, Korovin S D, Rostov V V, Pegel I V, Mesyats G A, Rukin S N, Shpak V G, Yalandin M I and Ginzburg N S 2003 *Laser Part. Beams* **21** 187
[34] Korovin S D, Mesyats G A, Rostov V V, Ul'maskulov M R, Sharypov K A, Shpak V G, Shunailov S A and Yalandin M I 2004 *Tech. Phys. Lett*. **30** 117
[35] Klimov A I, Korovin S D, Rostov V V, Ulmaskulov M R, Shpak V G, Shunailov S A and Yalandin M I 2002 *IEEE T. Plasma Sci*. **30** 1120
[36] Grishin D M *et al* 2002 *Tech. Phys. Lett*. **28** 806
[37] Korovin S D, Litvinov E A, Mesyats G A, Murzakaev A M, Rostov V V, Shpak V G, Shunailov S A and Yalandin M I 2004 *Tech. Phys. Lett.* **30** 813
[38] Rostov V V, Yalandin M I and Mesyats G A 2008 *IEEE T. Plasma Sci*. **36** 655
[39] Yalandin M I, Reutova A G, Ul'maskulov M R, Sharypov K A, Shpak V G, Shunailov S A,

Klimov A I, Rostov V V and Mesyats G A 2009 *Tech. Phys. Lett.* **35** 804
[40] Rostov V V, Tsygankov R V, Vykhodsev P V, Konev V Y, Stepchenko A S 2021 *IEEE Electr. Device L.* **42** 935
[41] Rostov V V, El'chaninov A A, Klimov A I, Konev V Yu, Romanchenko I V, Sharypov K A, Shunailov S A, Ul'maskulov M R and Yalandin M 2013 *IEEE T. Plasma Sci*. **41** 2735
[42] Ginzburg N S *et al* 2015 *Phys. Rev. Lett*. **115** 114802
[43] Mesyats G A *et al* 2017 *Phys. Rev. Lett*. **118** 264801
[44] Ginzburg N S, Golovanov A A, Romanchenko I V, Rostov V V, Sharypov K A, Shunailov S A, Ulmaskulov M R, Yalandin M I and Zotova I V 2018 *J. Appl. Phys.* **124** 123303
[45] Sharypov K A, Shunailov S A, Ginzburg N S, Zotova I V, Romanchenko I V, Rostov V V, Ulmasculov M R, Shpak V G and Yalandin M I 2019 *Radiophys. Quant. El.* **62** 447
[46] Sharypov K A, Rostov V V, Sadykova A G, Shpak V G, Shunailov S A and Yalandin M I 2018 *Appl. Phys. Lett*. **113** 223502
[47] Shunailov S A, Mesyats G A, Romanchenko I V, Rostov V V, Sadykova A G, Sharypov K A, Shpak V G, Ulmasculov M R, and Yalandin M I 2019 *J. Appl. Phys*. **126** 164504
[48] Yalandin M I, Shunailov S A, Ul'maskulov M R, Sharypov K A, Shpak V G, Rostov V V, Romanchenko I V, El'chaninov A A and Klimov A I 2012 *Tech. Phys. Lett*. **38** 917
[49] Yalandin M I, Mesyats G A, Rostov V V, Sharypov K A, Shpak V G, Shunailov S A and Ulmaskulov M R 2008 *IEEE T. Plasma Sci*. **36** 2604
[50] Ginzburg N S, Zaslavsky V Yu, Malkin A M, Sergeev A S, Zotova I V, Sharypov K A, Shunailov S A, Shpak V G, Ul'masculov M R and Yalandin M I 2020 *Appl. Phys. Lett*. **127** 183505
[51] Rostov V V, Romanchenko I V, Pedos M S, Rukin S N, Sharypov K A, Shpak V G, Shunailov S A, Ul'masculov M R and Yalandin M I 2016 *Phys. Plasmas* **23** 093103